Journal of Applied Mechanics and Technical Physics, Vol. 44, No. 2, pp. 221–227, 2003

VELOCITY MEASUREMENTS IN A ONE-DIMENSIONAL STEADY FLOW BY METHODS OF EMISSION TOMOGRAPHY

A. V. Likhachev

UDC 533.9+518.517.948+533.605

A new method for velocity-field measurements in a one-dimensional steady flow is proposed. The method is based on principles of laser-induced fluorescence combined with emission tomography. Results of a numerical experiment are presented.

Key words: *emission tomography, flow diagnostics, laser-induced fluorescence.*

INTRODUCTION

The velocity field in a flow is usually measured by laser anemometers (see, e.g., [1–3]). These instruments generate a probing interference field in the flow region under study. The measurement includes the formation of an image or Fourier image of this field in diffuse light, its subsequent transformation into an electric signal, and analysis. The problems of light scattering by particles moving with the flow were considered, in particular, in [4, 5]. Algorithms of signal processing in laser anemometry are discussed in [6]. It should be noted that high-speed photographing is sometimes used in diagnostic methods to determine consecutive positions of particles entrained by the flow [7]. Some new results in the field of flow-velocity measurements can be found in [8].

The following experimental layout is described in [9]. A certain cross section is selected in the flow by a laser sheet. A frequency-tuned laser is used, which allows one to achieve resonant absorption of radiation in the selected layer by molecules (or radicals) of a certain type. Then, the Doppler shift of fluorescence caused by collective motion of excited molecules in the flow is registered.

The method of velocity-field measurement in a one-dimensional steady flow, proposed in the present paper, is similar to the above-described method of planar laser-induced fluorescence; as in [9], molecules in one cross section are excited, but the fluorescence signal rather than the Doppler shift is further analyzed, because the former is much simpler to measure. Under certain conditions, the velocity field is uniquely related to the spatial distribution of excited molecules. In turn, this distribution can be found by measuring the integral intensity of fluorescence. The method has been tested by a numerical experiment.

1. DERIVATION OF AN EQUATION RELATING THE VELOCITY OF A ONE-DIMENSIONAL GAS FLOW WITH THE CONCENTRATION OF EXCITED MOLECULES

Let the velocity of an examined steady flow (for certainty, a gas flow is considered) have only one component $v_z \equiv v(x, y, z)$ (the subscript is omitted later on). The following method is proposed to determine the field $v(x, y, z)$. Let the molecules in the beginning of the flow section considered ($z = 0$) in a thin layer dz be converted to an excited state during a negligibly small time by some agent (e.g., laser sheet). We assume this moment to be the initial time. Let n_0 be the concentration of excited molecules at the initial time. We consider a small volume ΔV located in a vicinity of the point $(x_0, y_0, 0)$ at $t = 0$. At later times, this volume moves along a streamline parallel,

Institute of Theoretical and Applied Mechanics, Siberian Division, Russian Academy of Sciences, Novosibirsk 630090. Translated from Prikladnaya Mekhanika i Tekhnicheskaya Fizika, Vol. 44, No. 2, pp. 83–91, March–April, 2003. Original article submitted May 7, 2002; revision submitted July 29, 2002.

0021-8944/03/4402-0221 $25.00

by condition, to the z axis. We assume that the diffusion velocity of molecules is much lower than the velocity of their collective motion in the flow and the flow velocity, in turn, is much lower than the velocity of sound, i.e., the gas can be considered as incompressible. Under these assumptions, the number of excited molecules in the volume ΔV in the course of its motion is mainly reduced due to relaxation of the molecules to the ground state. If the gas is sufficiently rarefied, the main mechanism of relaxation is spontaneous radiation. Then, we can write the relation

$$N(x_0, y_0, z) = n_0 \Delta V \exp(-\alpha t), \tag{1}$$

where α is a constant characterizing the relaxation velocity of the molecules to the ground state. The time t in Eq. (1) can be expressed via the current coordinate of the volume ΔV and flow velocity. The latter, due to flow steadiness, depends on the position of the point on the streamline only:

$$t = \int_0^z \frac{dz'}{v(x_0, y_0, z')}. \tag{2}$$

Substituting (2) into (1) and using some simple transformations, we obtain

$$\int_0^z \frac{dz'}{v(x_0, y_0, z')} = \frac{1}{\alpha} \ln \frac{n_0 \Delta V}{N(x_0, y_0, z)}. \tag{3}$$

Passing in (3) to the limit $\Delta V \to 0$, we have, in the logarithm expression, the ratio of the concentration of the excited molecules at the initial time in the plane $z = 0$ to their concentration $n(x_0, y_0, z)$ at the point (x_0, y_0, z) at the time determined by Eq. (2). Differentiating Eq. (3) with respect to z, we obtain

$$v(x_0, y_0, z) = -2\alpha n(x_0, y_0, z) \Big(\frac{\partial n(x_0, y_0, z)}{\partial z} \Big)^{-1}. \tag{4}$$

Expression (4) describes the velocity of one-dimensional motion of the gas on the streamline $x \equiv x_0$, $y \equiv y_0$.

2. DETERMINATION OF THE CONCENTRATION OF EXCITED MOLECULES BY THE TOMOGRAPHY METHOD

Knowing the concentration of excited molecules $n(x, y, z)$, Eq. (4) yields the flow velocity at every point. Generally speaking, the concentration $n(x, y, z)$ in Eq. (4) is taken at different times for different z coordinates. Under the assumption adopted, however, excitation is performed in a thin layer, which is assumed to be a plane. In accordance with the flow model considered, this plane is further divided into individual sectors, each of them moving with its own velocity along the streamlines (Fig. 1). Therefore, radiation at each point occurs at one time only. This allows us to ignore the time dependence in Eq. (4) and seek the concentration $n(x, y, z)$ as a purely spatial distribution, though it is dynamic in reality.

The problem of determining $n(x, y, z)$ can be solved by methods of computerized tomography. Transition of molecules to the ground state gives rise to fluorescence whose intensity is proportional to molecular concentration. The measurement scheme is shown in Fig. 2. Several two-dimensional detectors registering mainly radiation incident perpendicular to their surface are located parallel to the flow centerline at different azimuthal angles. The length of the detectors is assumed to be sufficient to obtain data within the entire volume under study. As the sectors of the surface initially belonging to the plane $z = 0$ move, the detectors register the "traces" of these sectors, whose brightness in the downstream direction decreases with decreasing number of excited molecules.

We assume that the processes of radiation absorption and scattering can be neglected. Within the framework of the above assumptions, the signal registered at a certain point of the detector inclined at an angle φ to the x axis can be represented by the equation

$$f(p, z) = k \int_{S_1}^{S_2} n(s\cos\varphi + p\sin\varphi, s\sin\varphi + p\cos\varphi, z)\, ds. \tag{5}$$

Here p is the coordinate on the detector in the direction perpendicular to the z axis, S_1 and S_2 are intersection points of the beam along which observation is performed with flow boundaries, and k is a coefficient depending on particular test conditions. The distribution of signal intensity on the detector surface $f(p, z)$ is called a two-dimensional projection.

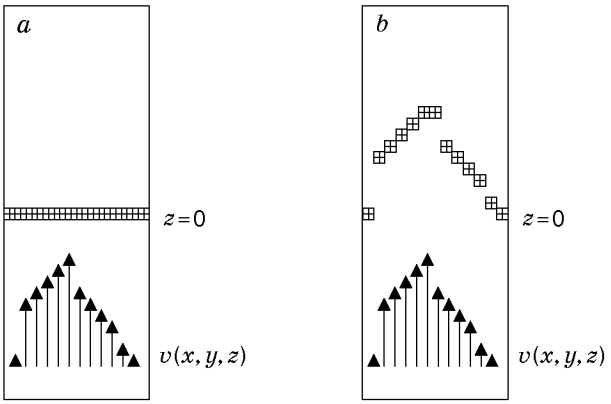

Fig. 1

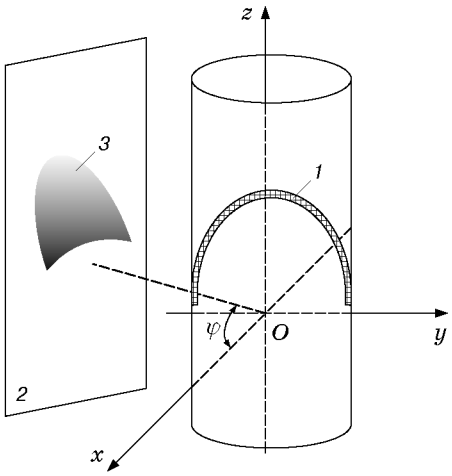

Fig. 2

Fig. 1. Distribution of excited molecules immediately after excitation (a) and at some subsequent moment (b).

Fig. 2. Measurement scheme: 1) envelope of the front of motion of excited molecules in the flow; 2) two-dimensional detector; 3) signal registered by the detector.

Equations similar to (5) form the basis for emission tomography of self-luminous objects [9, 10]. Let there be projection data f obtained by measurements. The relation between f and the distribution examined [in our case, the distribution of the concentration of excited molecules $n(x, y, z)$] is described by a known integral operator. In the beam-tomography approximation considered, this operator is specified by Eq. (5), i.e., the signal at each point of the detector is put into correspondence to the integral of $n(x, y, z)$ along a certain straight line. The problem of tomography is to find the unknown function $n(x, y, z)$ using the data f. Many algorithms have been developed to solve this problem (see, e.g., [11–13]).

Tomographic reconstruction requires a rather large number of measurements. If the data are united into two-dimensional projections, the latter should be registered at several angles with respect to the object. In practice, the measurement scheme is often subjected to constraints, including that on the number of observation directions. The reason can be complexity of equipment or insufficient availability of the object (for instance, a flow inside a tube). If the amount of known data is insufficient, the unknown function is usually reconstructed using algebraic methods [11]. As a result of discretization, the sought vector $\boldsymbol{n} \in \boldsymbol{R}^J$ turns out to be related to the measurement vector $\boldsymbol{f} \in \boldsymbol{R}^I$ by a system of linear algebraic equations $A\boldsymbol{n} = \boldsymbol{f}$. In the beam-tomography approximation, the matrix element a_{ij} is often defined as the length of intersection of the ith beam with the jth voxel. (Voxels are elementary volumes into which the reconstruction domain is divided during discretization.) Therefore, the matrix A is rather sparse. There are special iterative algorithms to solve systems of linear algebraic equations of this kind. In our computational experiment, we used the algebraic reconstruction technique (ART). According to [11], the $(k+1)$th step in ART is defined by the formula

$$\boldsymbol{n}^{(k+1)} = \boldsymbol{n}^{(k)} + \lambda \frac{f_{i(k)} - (\boldsymbol{a}^{i(k)}, \boldsymbol{n}^{(k)})}{\|\boldsymbol{a}^{i(k)}\|} \boldsymbol{a}^{i(k)}. \tag{6}$$

Here $\boldsymbol{a}^{i(k)}$ is the ith row of the matrix A, λ is the relaxation parameter, $i(k) = k(\mathrm{mod}\, I) + 1$, i.e., the matrix rows are handled in a cyclic manner, $(\cdot, \cdot)$ indicates a scalar product, and $\|\cdot\|$ is the Euclidean norm in $\boldsymbol{R}^J$. It was shown [11] that process (6) converges for all initial approximations $\boldsymbol{n}^{(0)} \in \boldsymbol{R}^J$ if $0 < \lambda < 2$. If, in addition, the approximation $\boldsymbol{n}^{(0)}$ belongs to the linear shell of the vectors $\boldsymbol{a}^{(i)}$, $i = 1, \ldots, I$, then the iterations converge to the solution of the system of equations with a minimum norm for a compatible system and to the generalized solution for an incompatible system.

Thus, using the proposed experimental technique involving emission tomography, one can reconstruct the dynamic distribution of the concentration of excited molecules from the measured values of integral fluorescence. At the same time, knowing this distribution, one can calculate the velocity field of the one-dimensional steady flow under study using formula (4).

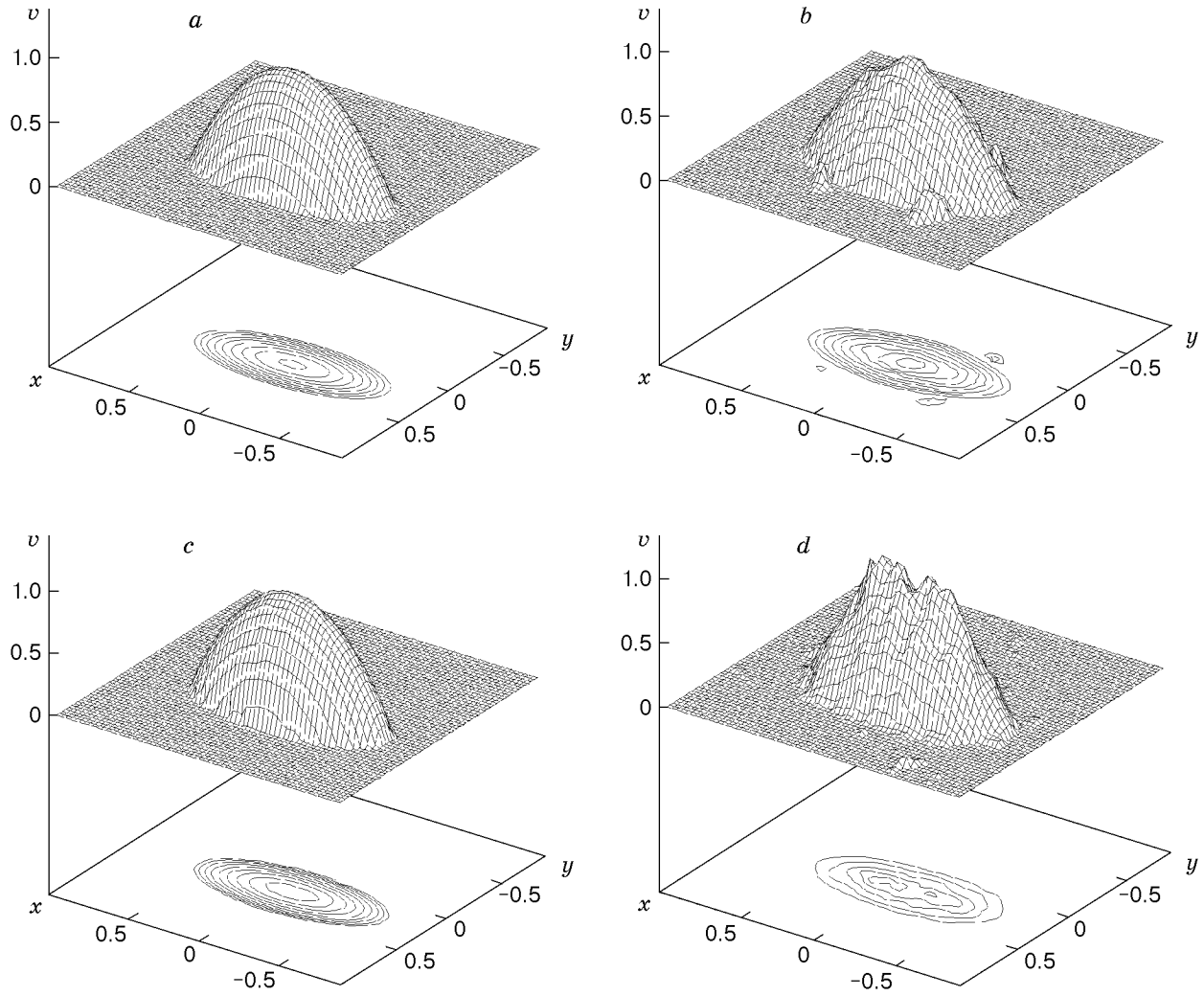

Fig. 3. Cross section of the velocity field by the plane $z = 0.2$: exact model (a) and results of reconstruction (b–d); (b) $\alpha = 0.5$, the number of projections $K = 5$, and $\Delta = 0.176$; (c) $\alpha = 0.5$, $K = 15$, and $\Delta = 0.091$; (d) $\alpha = 0.5$, $K = 6$, random noise in projection data $\xi = 6\%$, and $\Delta = 0.272$.

3. NUMERICAL EXPERIMENT

3.1. Description of Models. The method developed was tested in a numerical experiment. The following velocity distribution $v(x, y, z)$ was initially set:

$$v(x,y,z) = \frac{v_0}{\sqrt{z+z_0}}\Big(1 - \frac{(x-X_c)^2}{a^2} - \frac{(y-Y_c)^2}{b^2}\Big), \quad \frac{(x-X_c)^2}{a^2} + \frac{(y-Y_c)^2}{b^2} \leqslant 1, \quad z > 0. \tag{7}$$

In computations, we used conventional units based on which the parameters in Eq. (7) had the following values: $v_0 = 1$, $z_0 = 2$, $a = 0.25$, $b = 0.7$, $X_c = -0.2$, and $Y_c = 0.1$. The cross section of the velocity field by the plane $z = 0.2$ is shown in Fig. 3a. Since the objective of the computational experiment was testing the method efficiency, the possibility of actual realization of the velocity field (7) was not considered. Nevertheless, formula (7) describes the main features of motion of a viscous gas in a vertical tube with an elliptic cross section in a gravity field.

Based on the prescribed velocity distribution, we calculated the concentration of excited molecules at different points of the flow. For this purpose, the expression for time (2) was substituted into Eq. (1) using dependence (7). As a result, we obtain the expression

$$n(x,y,z) = n_0 \exp\Big(-\frac{2\alpha z^2}{v_0(\sqrt{z+z_0}-\sqrt{z_0}\,)}\Big(1-\frac{(x-X_c)^2}{a^2}-\frac{(y-Y_c)^2}{b^2}\Big)^{-1}\Big),$$
$$(x-X_c)^2/a^2+(y-Y_c)^2/b^2 \leqslant 1, \qquad z>0. \tag{8}$$

Then, we calculated the projection data (5); the distribution of the concentration of excited molecules corresponded to Eq. (8). The coefficients k and n_0 were assumed to be equal to unity. Thus, detector readings were simulated. Based on these data, the distribution $n(x,y,z)$ was simulated using the ART algorithm (6). Then, the dependence $n(x,y,z)$ was substituted into Eq. (4) used to calculate the velocity field.

Distributions (7) and (8) were calculated on a grid with $129\times129\times129$ nodes, specified in a cube with the center at the origin and the edge length equal to two conventional units. Reconstruction was performed on the same grid. On two-dimensional projections (detectors), a grid 129×129 was defined, with integral (5) calculated for each node.

The velocity field reconstructed by the above-described technique was compared to the model velocity field determined by Eq. (7). The normalized root-mean-square error Δ was calculated by the formula

$$\Delta = \sqrt{\sum_{j=1}^{J}(v_j-v_j^r)^2}\Big/\sqrt{\sum_{j=1}^{J}(v_j)^2}, \tag{9}$$

where v and v^r are the model and reconstructed velocity fields, respectively; summation is performed over grid nodes in the three-dimensional space. The accuracy of tomographic reconstruction of the concentration of excited molecules was also characterized by the error Δ determined similar to (9).

3.2. Effect of the Parameter α on the Magnitude of the Reconstruction Error. The length of the flow sector in which the velocity field can be calculated depends on the residence time of molecules in the excited state, which is characterized by the parameter α. Under conditions of a real experiment, it is difficult to vary this parameter, because it is determined by the type of the fluorescent substance. Therefore, we have to estimate the length L of the sector where the velocity can be reconstructed with sufficient accuracy for a given α. The estimate $L\sim U/\alpha$ is very rough. The effect of α is studied in the numerical experiment.

On one hand, the distribution $n(x,y,z)$ depends on α, which can affect the accuracy of solving the tomographic problem based on the projection data (5); on the other hand, α enters into Eq. (4), where the velocity is expressed via the concentration of excited molecules. The contributions of these effects to the root-mean-square error were considered separately and together. For convenience, in the present series of computations, we fixed the value of L (because it is determined by the model size) and varied the value of α.

Curves 1 and 2 in Fig. 4 show the effect of the parameter α on the error Δ in calculating $v(x,y,z)$ from Eq. (4). The distribution $n(x,y,z)$ is not reconstructed on the basis of the projection data (5) but is calculated directly using Eq. (8). In other words, curves 1 and 2 show the accuracy of solving Eq. (3) using formula (4). The derivative in Eq. (4) was taken numerically, since the analytical expression for $n(x,y,z)$, generally speaking, is unknown in real experiments. Numerical determination of the derivative is an ill-posed problem. Therefore, in the case of distortion of the function $n(x,y,z)$ by random noise (see below), it was smoothed by a one-dimensional median filter with respect to the variable z. The difference between curve 1 and curve 2 is that 3% noise was superimposed on the array $n(x,y,z)$ in constructing curve 2. It follows from Fig. 4 that noise significantly decreases the accuracy of velocity-field reconstruction, especially at large values of α.

Curve 3 in Fig. 4 refers to the complete solution of the problem. Using Eq. (8), we calculated the concentration of excited molecules $n(x,y,z)$ for a given value of the parameter α. According to (5), we determined six projections at angles $\varphi = 0$, 30, 60, 90, 120, and 150°. Based on these data, tomographic reconstruction was performed using algorithm (6); the result of this reconstruction was substituted into formula (4). The computations show that the accuracy of tomographic reconstruction of the function $n(x,y,z)$ from ideal (i.e., not distorted by random noise) projection data decreases only insignificantly with increasing α. Thus, in our case, the decrease in the accuracy of velocity-field reconstruction with increasing α is mainly caused by the low accuracy of solving Eq. (3).

3.3. Dependence of the Error on the Number of Two-Dimensional Projections. In the general case, the accuracy of tomographic reconstruction depends on the amount of projection data (in the formulation considered, on the number of two-dimensional projections K). Hence, the error in velocity-field reconstruction also depends on the number of observation directions.

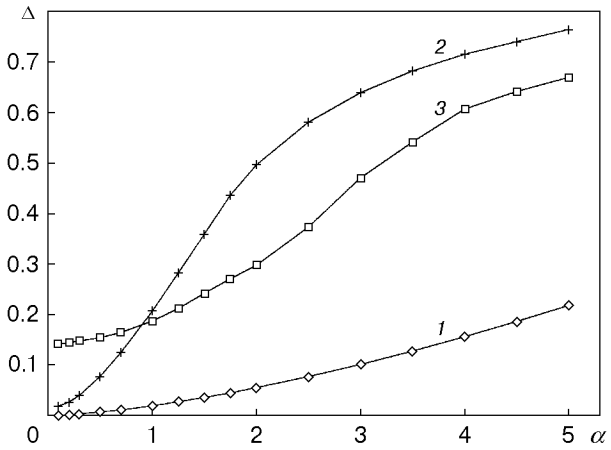

Fig. 4

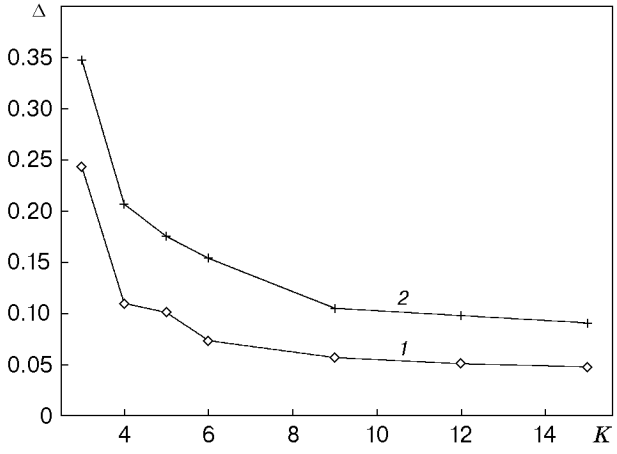

Fig. 5

Fig. 4. Error Δ versus the parameter α: curve 1 shown the solution of Eq. (3) with the use of Eqs. (4) and (8); curve 2 shows the same solution for $\xi = 3\%$; curve 3 shows the complete solution of the problem with the use of six projections.

Fig. 5. Error Δ versus the number of projections K for $\alpha = 0.5$: curve 1 shows the error of reconstructing the distribution $n(x, y, z)$; curve 2 shows the error of reconstructing the velocity field, based on the reconstructed function $n(x, y, z)$.

Figure 5 shows the dependences of Δ on the number of projections K. The projections were distributed uniformly over the angle φ in the interval from 0 to 180°. The computations were performed for $\alpha = 0.5$. Curve 1 shows the dependence of the error of tomographic reconstruction of the distribution $n(x, y, z)$ on the number of projections K, which was obtained using algorithm (6). Curve 2 shows the error of velocity-field reconstruction, by means of Eq. (4), from reconstructed distributions of excited molecules. It is seen that the accuracy of solving the problem increases insignificantly for $K > 9$. The reason is the effect of saturation in terms of the number of observation directions, typical of algebraic methods of tomographic reconstruction (including the ART algorithm).

The accuracy of velocity-field reconstruction for different numbers of observation directions can be qualitatively estimated using Fig. 3b and c, which shows the cross sections by the plane $z = 0.2$.

3.4. Random Noise in Projection Data. As is noted in Sec. 3.2, distortions in the distribution $n(x, y, z)$ significantly worsen the accuracy of velocity-field reconstruction. In the formulation considered, the function $n(x, y, z)$ is distorted by artefacts of tomographic reconstruction caused, in particular, by the small number of projections and by random noise always present in projection data in practice. The effect of noise is considered below in more detail.

The noise was assumed to have a Gaussian distribution with the mean equal to zero. The ratio ξ of noise dispersion to the maximum value of the signal for each projection was constant. In the case of noisy data, regularization procedures were used in solving the problem. For tomographic reconstruction of the distribution of excited molecules $n(x, y, z)$, the ART algorithm included a smoothing adaptive frequency filter [12]. In reconstructing the velocity field by Eq. (4), the function $n(x, y, z)$ was smoothed by a one-dimensional median filter with respect to the variable z. Depending on noise intensity, the filter length was varied from three to nine points.

Figure 6 shows the dependences $\Delta(\xi)$. Note the difference between curves 2 in Figs. 4 and 6. In the first case, the function $n(x, y, z)$ calculated by Eq. (8) was distorted. In the second case, the noise was applied onto the projection data (5) used to reconstruct the dependence $n(x, y, z)$. It follows from Fig. 6 that the tomographic reconstruction of the distribution $n(x, y, z)$ and the reconstructed velocity field $v(x, y, z)$ are rather stable to noise within the range examined if regularization procedures are used.

Figure 3d shows the cross section of the velocity field reconstructed from noisy initial data by the plane $z = 0.2$.

CONCLUSIONS

The proposed method for determining the velocity field of a one-dimensional steady flow is rather simple in experimental implementation because it does not require complicated spectroscopic and interference measurements.

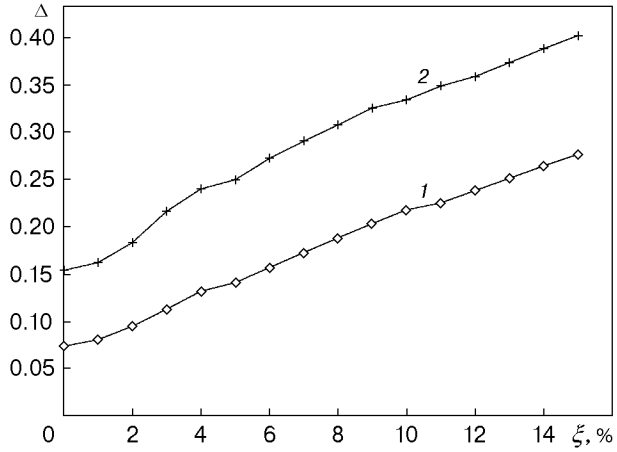

Fig. 6. Error Δ versus the noise level ξ for $\alpha = 0.5$ and $K = 6$ (notation the same as in Fig. 5.)

The advantage of the method is also the possibility of determining the velocity over the entire length of the sector examined. The numerical experiment revealed rather high accuracy of velocity-distribution reconstruction. If the lifetime of molecules in the excited state is rather large, the root-mean-square error is less than 20% for five or six observation directions.

The drawback of the method is that it can be applied in the above-described form to a limited class of flows only. In prospects, however, the range of applicability of the method can be extended, in particular, to unsteady flows. The distribution of excited molecules will still be found by solving the emission-tomography problem, but the relation between this distribution and velocity field will be determined by an equation more complicated than Eq. (4).

The author is grateful to V. V. Pickalov for discussion of the work and valuable comments.

REFERENCES

1. Yu. N. Dubnishchev and B. S. Rinkevichus, *Methods of Laser Doppler Anemometry* [in Russian], Nauka, Moscow (1982).
2. B. S. Rinkevichus, *Laser Diagnostics of Flows* [in Russian], Izd. Mosk. Énerg. Inst., Moscow (1990).
3. I. V. Basargin, G. I. Mishin, and I. P. Yavor, "Spectral methods in ballistic experiment," in: *Optical Methods in Ballistic Experiment* (collected scientific papers) [in Russian], Nauka, Leningrad (1979), pp. 114–129.
4. R. J. Adrian and K. L. Orloff, "Laser anemometer signals: visibility characteristics and applications to particle sizing," *Appl. Optics*, **16**, No. 3, 677–684 (1977).
5. Yu. N. Dubnishchev, "Effect of the size of scattering particles on the signal in laser velocimeters with a probing interference field," *Kvant. Élektron.*, **22**, No. 12, 1262–1266 (1995).
6. V. A. Grechikhin and B. S. Rinkevichus, "Digital methods of signal processing in laser anemometry and vibrometry," *Avtometriya*, No. 1, 59–67 (1999).
7. V. M. Boiko, V. V. Pickalov, S. V. Poplavski, and N. V. Chugunova, "Determination of the gas parameters in nonrelaxing two-phase flow on dynamics of admixture particles," in: *Proc. of the 10th Int. Conf. on the Methods of Aerophysical Research*, Part 1 (Novosibirsk, July 9–15, 2000), Izd. Sib. Otd. Ross. Akad. Nauk, Novosibirsk (2000), pp. 31–36.
8. *Optical Methods of Flow Research*: Proc. VI Int. Conf. (Moscow, June 27–29, 2001), Izd. Mosk. Énerg. Inst., Moscow (2001).
9. V. V. Pickalov and N. G. Preobrazhenskii, *Reconstruction Tomography in Gas Dynamics and Plasma Physics* [in Russian], Nauka, Novosibirsk (1987).
10. V. V. Pickalov and T. S. Mel'nikova, *Plasma Tomography* [in Russian], Nauka, Novosibirsk (1995).
11. G. T. Herman, *Image Reconstruction from Projections: The Fundamentals of Computerized Tomography*, Academic Press, New York (1980).
12. A. V. Likhachev and V. V. Pickalov, "Frequency filtration in algebraic algorithms of three-dimensional tomography," *Avtometriya*, No. 4, 83–89 (1995).
13. A. V. Likhachev and V. V. Pickalov, "Synthesized algorithm of three-dimensional tomography," *Mat. Model.*, **10**, No. 1, 73–85 (1998).